ISSN 1330–0008
CODEN FIZAE4

TEMPERATURE AND POWER-DEPENDENT MEASUREMENTS OF Rb D_2 TRANSITIONS BY DOPPLER-LIMITED AND DOPPLER-FREE SPECTROSCOPY

DIPANKAR BHATTACHARYYA, BIBHAS K. DUTTA, BISWAJIT RAY AND PRADIP N. GHOSH

Department of Physics, University of Calcutta, 92, A. P. C. Road, Calcutta – 700 009, India
e-mail: png@cubmb.ernet.in

Received 23 March 2003; revised manuscript received 17 September 2003
Accepted 29 September 2003 Online 19 April 2004

An external-cavity diode-laser spectrometer has been set up for high-resolution measurement of line shapes of the Rb D_2 transitions. Temperature-dependent fine-structure measurements are carried out in a free-running temperature condition by using frequency ramps for repetitive current tuning over a region of 17 GHz, encompassing all of the four Doppler broadened transitions of the two isotopes in an almost collision-free region. The Doppler broadened widths extracted from temperature-dependent line shapes, on least squares fitting to observed data, lead to an estimation of root-means-square velocities of vapour atoms under varying temperature conditions. Saturated-absorption spectroscopic measurements show complete resolution of the hyperfine Lamb dips and crossover resonance dips of one ^{87}Rb D_2 transition. Data recorded from power-dependent measurement of one unresolved ^{85}Rb D_2 transitions are analyzed to obtain the saturation parameter and power broadening coefficient. The linewidths of different fully resolved Lamb dips of the hyperfine and crossover–resonance components are not the same, suggesting differences in their natural linewidths.

PACS numbers: 42.62.Fi, 33.70.-w, 33.70.Jg UDC 539.186

Keywords: diode laser spectroscopy, Rb D_2 transitions, temperature dependent line shape, saturation spectroscopy, hyperfine spectra

1. Introduction

Spectroscopic studies of Rb D_2 transitions are of great importance because of the suitability of Rb in laser cooling [1] and Bose–Einstein condensation [2]. A large number of hyperfine structure and other measurements on Rb D_2 transitions have been reported [3–6]. Line shape studies of Doppler broadened components of seeded atomic Rb D_2 transitions were carried out at high kinetic temperature of 900 – 1400 K at high repetitive scan-rate (15 kHz) over 1 – 3 cm^{-1}. These results show the reliability of Rb absorption spectroscopy in optical diagnostics of hypersonic airflows. On the other hand, temperature-dependent measurements of Gaussian line shapes are used as indicators of kinetic temperature at extremely low temperatures before the formation of Bose–Einstein condensation [2]. Hence, a measurement of Gaussian line shapes in an almost collision-free region at a low pressure of the order of μtorr in a free-running temperature condition would display the instantaneous change in atomic velocities as a function of temperature. In order to estimate the Lorentzian component in the measured Doppler broadened line profile, investigation of saturated absorption spectra under similar thermal conditions is a prerequisite. In the collision-free region, the Lorentzian components arise from the natural broadening, power broadening, transit time broadening and the contributions from laser linewidth and detector noise. A careful investigation of the spectral line profiles at varied power and temperature may lead to apportioning the line-shape contributions originating from different mechanisms.

Diode lasers have played a dominant role in atomic physics over the last two decades [7]. Simple operation, low cost, relatively easy tuning and modulation techniques have characterized the near-infrared diode lasers as a suitable replacement of dye lasers, particularly for high-resolution measurements and line-shape analysis in the visible to near-infrared region. High-resolution diode-laser spectroscopic measurements of atmospheric gases have demonstrated the efficiency of diode lasers to obtain useful data on line intensity and broadening parameters from line-shape analysis [8–11]. For high-resolution saturation spectroscopy, external-cavity diode laser with linewidth of the order of 1 MHz is necessary [12–13]. The temperature dependence of Doppler broadened D_1 transitions of K has been discussed qualitatively in Ref. [12].

We report measurements of the effect of temperature variation on the Doppler-broadened profiles of D_2 transitions of ^{85}Rb and ^{87}Rb in the free-running temperature conditions. The broadening parameters, like line intensity and linewidth, are retrieved by fitting the observed data points with the standard line profile. The root-mean-square velocities of Rb vapour atoms for two isotopes calculated from their measured linewidths are compared with their values computed from measured temperature. To our knowledge, a quantitative study of the temperature-dependent line shapes of Rb D_2 transitions at ambient temperatures has not been published so far. Effects of saturation or power broadening on spectral line shape is observed if the power of the laser beam is sufficient to cause the excited atom population to deviate from the equilibrium value existing in the absence of the laser beam. A counter-propagating probe beam encounters the hole in the population distribution curve of the lower state and leads to a dip in the Doppler-broadened absorption background. In addition to the Lamb dip, crossover resonances occur at intermediate frequencies when the probe transition of one hyperfine component crosses the hole created by a pump transition of a nearby hyperfine component sharing the same lower level [14,15]. The precise values of the saturation parameters with varied power of the saturating beam are extracted from the observed line shape and this leads to the power broadening coefficient. The contributions from different line broadening mechanisms on the observed line shape are discussed.

2. *Experimental*

An external cavity diode laser (ECDL) from New Focus, USA has been used for both Doppler broadened and saturated-absorption spectroscopic measurements. Figure 1 shows the schematic of the experimental setup used for the measurement of Doppler-free saturation spectroscopy. In order to detect Doppler-broadened line shapes, the mirror, M, in Fig. 1, placed beyond the Rb-cell is replaced by the silicon photodetector, i.e. the part of the laser beam transmitted by the cavity *via* the sample cell is directly focused onto the detector. All other accessories placed on the optical paths and the detection electronics are kept unchanged. A $\lambda/4$ plate has been used to prevent optical feedback which causes power and frequency instability of the laser emission. The GaAlAs semiconductor laser diode is used in Littman configuration in the ECDL system. At an operating drive current of 69 mA, the laser power emitted by the diode is 1.9 mW under ambient temperature conditions. The residual coarse tunability ($\geq$ 0.01 nm sec^{-1}) is obtained by shifting the tuning mirror attached to the piezoelectric transducer (PZT) driver in the external cavity of the diode laser system. By applying slowly-varying ramp voltage to the PZT-driver, fine input tunability of the order of 10 GHz/V is achieved. The Rb-cell used for this work is a cylindrical Pyrex-glass cell of 5 cm path length and 2.5 cm diameter. The beam diameter is 3 mm and remains unaltered in the optical paths before passing through the focusing lenses used for detection (Fig. 1). Part of the laser beam is fed to another photodetector through an air-spaced etalon from TecOptics for relative calibration of the frequency scale. As shown in Fig. 1, the laser power entering the sample cell is reduced by the beam split-

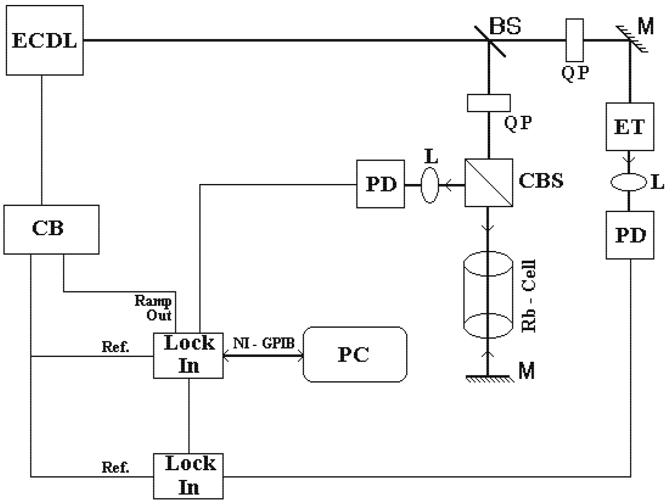

Fig. 1. Experimental setup for saturated-absorption measurement: ECDL – external cavity diode laser, CB – control box, PD – photo detector, L – convex lens, QP – quarter wave plate, BS – beam splitter, M – mirror, ET – etalon, PC – personal computer.

ters, quarter-wave ($\lambda/4$) plate and beam steering optics (not shown in the figure). The actual power density in the sample cell is less than 1 mW/cm^2. In order to observe the Doppler broadened transitions at a free-running temperature, the cell is heated by using incandescent lamps. The temperature monitoring is done by using a PT-100 thermocouple temperature sensor attached to the cell and a temperature controller. The process of heating the cell performed by passing electric current through a coil is not used in order to avoid the resultant magnetic field that can cause Zeeman shift. The diode laser injection current is modulated sinusoidally at a frequency of 5 kHz which is also supplied as a reference to the lock-in amplifier for 'in-phase' detection of the absorption signal. The transmitted power collected by the photodetector is sent to the lock-in amplifier SR530 interfaced to a personal computer *via* GPIB card from National Instruments. The lock-in time constant is set at 100 msec. The $1f$ detection technique has been adopted, leading to the first derivative output of the true absorption signals of the Rb D_2 transitions. The modulation amplitude has been adjusted so as to produce optimal signal having no undue broadening of the line. The energy level diagram in Fig. 2 shows the four Doppler-broadened transitions. Hyperfine splitting cannot be observed in this condition. Figure 3 shows the variations in the $1f$ Doppler-broadened signals with the increase in cell temperature for repeated ramp tuning. The ramp duration has been optimized to 30 sec. The temperature instability due to feeble fluctuation in

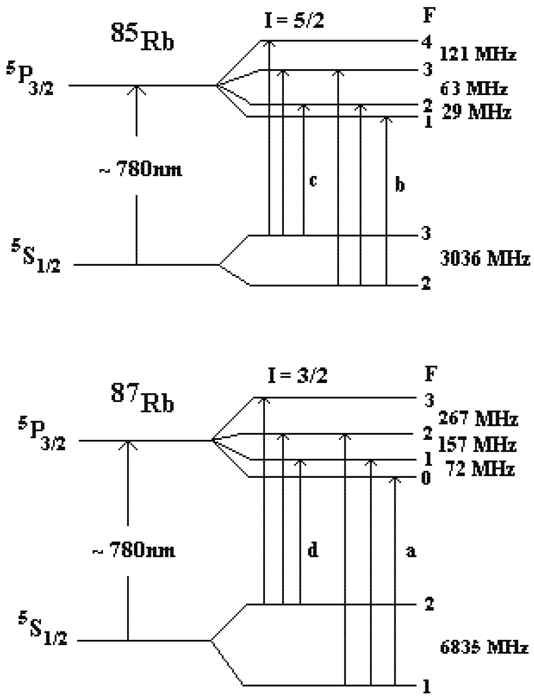

Fig. 2. Energy level diagram of hyperfine components in ^{85}Rb *and* ^{87}Rb D_2 *transitions.*

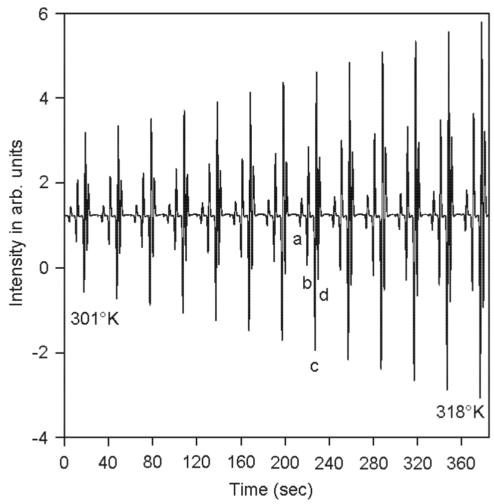

Fig. 3. Observed first derivative spectrum of Rb D_2 *transitions in free-running temperature condition. Transitions mentioned as (a), (b), (c) and (d) are designated in Fig. 2.*

the lamp power is limited to within ± 0.1 K. It may cause negligible change of less than 0.5% in the Doppler-broadened width. The base-line fluctuations arising from the noise of the heating source and the detector noise are minimized by applying the wavelength-modulation technique for 'in-phase' lock-in detection. The changes of linewidths with temperature are shown in Fig. 4. Since the atoms are heated

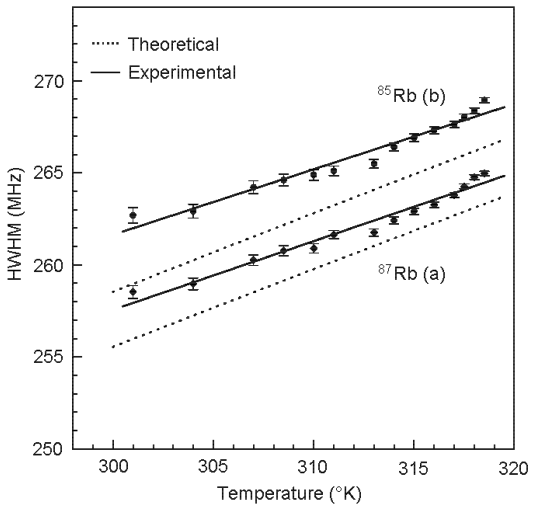

Fig. 4. Dependence of linewidth (HWHM), W_D on temperature for the ^{87}Rb *(marked (a) in Fig. 2) and* ^{85}Rb *(marked (b) in Fig. 2)* D_2 *transitions. The vertical-bars represent the standard errors obtained from the least-squares-fitting. The dotted curves show the corresponding computed theoretical values.*

continuously, the relative peak height and linewidth of any two lines within a ramp would be markedly different in different ramps (Fig. 3). We have noted the change in line shape of a particular transition in different ramps arising from a continuous increase of temperature at the moment the spectral line is recorded. In addition to the free-running temperature condition, we repeated the experiment by heating the cell to different temperatures within the measured range and keeping it at a stable temperature for a few minutes by using the temperature controller. No substantial change in the line shape was observed.

In the case of saturation-absorption spectroscopy, the part of the laser beam passing through the Rb-cell is retroreflected and finally focused onto the photodetector (Fig. 1). The cell is kept at room temperature (299 ± 0.1 K) throughout

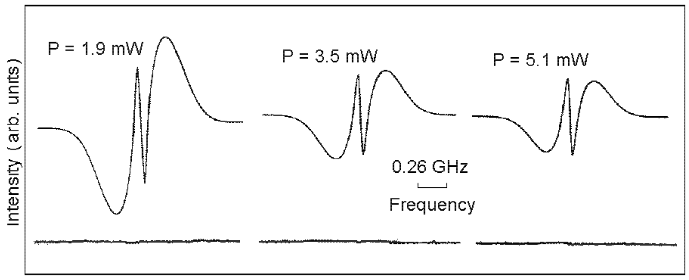

Fig. 5. Observed Lamb dip spectra for ^{85}Rb D$_2$ *transition* ($F_g = 2 \to F_e$) *at three laser powers. Intensities of the line profiles are given in arbitrary units. The lower traces plotted on the same scale as the observed line profile show the residuals of the observed and the least-squares fitted profiles.*

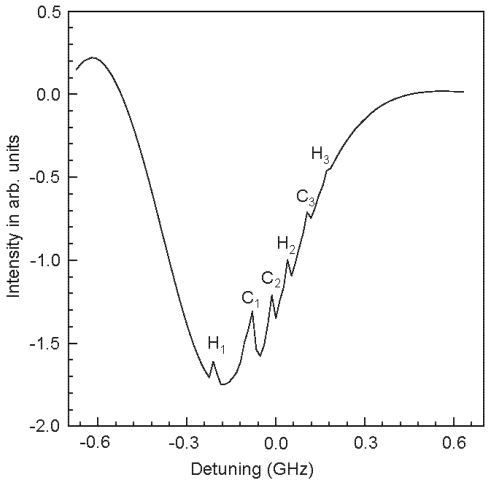

Fig. 6. Observed spectrum of Lamb dips with crossover resonances for ^{87}Rb D$_2$ *transition* ($F_g = 2 \to F_e$). H_1 ($F_g = 2 \to F_e = 3$), H_2 ($F_g = 2 \to F_e = 2$) *and* H_3 ($F_g = 2 \to F_e = 1$) *correspond to the hyperfine components and* C_1, C_2 *and* C_3 *are their respective crossover resonances.*

the experiment. The laser power is varied from 1.9 to 5.1 mW by changing the drive current. For three different powers, the measurement is repeated by keeping the other parameters unchanged. The power-dependent records of the unresolved ^{85}Rb D$_2$ transition ($F_g = 2 \rightarrow F_e = 1, 2, 3$) are shown in Fig. 5. The measured width (FWHM) of the order of 44 MHz of the unresolved saturated profile is somewhat smaller than the value of the width observed in Ref. [16]. The integrated profile of three Lamb dips and three crossover resonance components of ^{87}Rb D$_2$ transition ($F_g = 2 \rightarrow F_e = 1$, 2, 3) recorded at 1.9 mW laser power are shown in Fig. 6. Because of the larger hyperfine splitting of the upper level, all lines could be split.

3. *Results and discussion*

Transmission of the radiation through the sample cell is described by the Beer–Lambert's law,

$$I(\nu) = I_0 \exp\{-\kappa(\nu) L\}, \tag{1}$$

where I_0 is the unattenuated intensity of the source radiation, $I(\nu)$ is the radiation detected at the frequency ν, L is the length of the optical path within the cell and $\kappa(\nu)$ is the linear absorption coefficient, which can be expressed as

$$\kappa(\nu) = SN\alpha(\nu - \nu_0), \tag{2}$$

where S is the line intensity, N is the optical mass density and $\alpha(\nu - \nu_0)$ is the normalised line shape function around the line centre ν_0. Line intensity, S, in Eq. (2), has usually a strong correlation with the linewidth in the line shape function, $\alpha(\nu - \nu_0)$.

3.1. *Doppler-broadened transitions*

To extract the line shape parameters, a non-linear least-squares-fitting method, based on Levenberg–Marquardt procedure [17], is used for simulation of the observed data points of the first derivative spectrum for ^{85}Rb ($F_g = 2 \rightarrow F_e$) and ^{87}Rb ($F_g = 1 \rightarrow F_e$) D$_2$ transitions. The vapour pressure of the order of μTorr gives rise to the number of atoms per unit volume of the order of 10^{11} cm^{-3}. In this range of sample pressure, the effect of pressure broadening, of the order of 10^{-6} MHz, is negligible. Contributions to the Lorentzian component from other effects are small, as discussed in Sect. 3.2. So the line shape function in Eq. (2) can be approximated by a Gaussian. We have used the Doppler profile as the fitting function

$$\alpha_{\mathrm{D}}(\nu - \nu_0) = \frac{1}{W_{\mathrm{D}}} \sqrt{\frac{\ln 2}{\pi}} \exp\left\{ -\ln 2 \left(\frac{\nu - \nu_0}{W_{\mathrm{D}}} \right)^2 \right\}. \tag{3}$$

where the Doppler width (HWHM) is given by

$$W_{\mathrm{D}} = (\nu_0/c)\sqrt{2k_{\mathrm{B}} N_{\mathrm{A}} T \ln 2 / M}\,, \tag{4}$$

where k_B is the Boltzmann constant, N_A is the Avogadro's number, T is the temperature in Kelvin, c is the velocity of light and M is the atomic weight of the absorbing atom. The Doppler width (HWHM), W_D, and line intensity, S, are the fitting parameters. The normalised line intensity, S, is of the order of 1.109×10^{-23} cm molecule^{-1} for ^{85}Rb ($F_g = 2 \to F_e$) and 0.234×10^{-23} cm molecule^{-1} for ^{87}Rb ($F_g = 1 \to F_e$) D_2 transitions. We obtained temperature dependent data at thirteen temperatures in the range of 310 – 319 K. The HWHM obtained from the least-squares fitted curves are presented in Fig. 4 with their uncertainties. The fitted curve for HWHM against temperature shows a nearly $\sqrt{T}$ dependence, as expected from the theory. It may noticed that the measured half-widths are consistently above the computed values at different temperatures and this is beyond the limit of experimental uncertainty. The values of root-mean-square velocities of the Rb-isotopes for the above two transitions, estimated from the fitted Gaussian linewidths (HWHM), are listed in Table 1 for different temperatures. The measured values of the velocities are also compared with their theoretically predicted values. In both

TABLE 1. Observed and calculated values of root-mean-square velocities of ^{85}Rb *and* ^{87}Rb *atoms for* ($F_g = 2 \to F_e$) *and* ($F_g = 1 \to F_e$) D_2 *transitions, respectively. The numbers in parentheses are one standard deviations in units of the least significant digits.*

Temperature (K)	$v_{\rm rms}$ (m sec^{-1})			
	^{85}Rb		^{87}Rb	
	Obs.	Calc.	Obs.	Calc.
301.0	301.43(42)	297.15	296.65(34)	293.72
304.0	301.68(38)	298.63	297.15(32)	295.18
307.0	303.17(35)	300.10	298.63(29)	296.63
309.0	303.62(32)	301.08	299.23(27)	297.60
310.0	303.94(29)	301.56	299.37(25)	298.08
311.0	304.20(26)	302.05	300.23(22)	298.56
313.0	304.63(24)	303.02	300.35(20)	299.52
314.0	305.69(22)	303.50	301.11(19)	299.99
315.0	306.26(20)	303.99	301.67(17)	300.47
316.0	306.73(18)	304.47	302.07(16)	300.95
317.0	307.08(17)	304.95	302.68(14)	301.42
318.0	307.94(15)	305.43	303.81(13)	301.90
319.0	308.60(14)	305.91	304.04(12)	302.37

cases, theoretical values are lower than the observed values. Although the Doppler-broadened component could be fitted very well by Gaussian function, a convolution of the Lorentzian component that may arise from the residual power broadening originating from the power density of 1 mW/cm^2 with the Doppler-broadened Gaussian profile would lead to the smaller Doppler HWHM, i.e., smaller values of the root-mean-square velocities of the vapour atoms. Thus the actual temperature attained by the atoms is close to the temperature measured at the surface of the cell.

3.2. Doppler-free transitions

The spectrum of ^{87}Rb ($F_g = 2 \to F_e = 1, 2, 3$) hyperfine transitions (Fig. 6) leads to an estimation of the Lorentzian width (HWHM) of the Lamb dip spectra of the order of 10 MHz. This originates from natural linewidth of the transition, the instrumental width including laser linewidth, power broadened width, transit-time broadening and other non-predominant homogeneous broadening effects. The linewidth (HWHM) arising from transit time broadening

$$\Gamma_T = 7.06446\times 10^4 \frac{V_{avg}}{c\,D} \quad (\mathrm{MHz})\,, \tag{5}$$

where V_{avg} is the average velocity of the absorbing atoms, c is the velocity of light and D is the effective beam diameter within the sample cell, of the order of 0.023 MHz. The natural linewidth (FWHM) of each transition is of the order of 8 MHz [13]. To estimate the contribution of power-broadening effect to the linewidth, we have chosen unresolved symmetric Lamb-dip profile for ^{85}Rb ($F_g = 2 \to F_e$) transition. Simulation of saturated-absorption profile of this transition at three different laser powers will give rise to the power-broadening effect at different laser powers. We have used the Voigt-type line-shape function of the following form [18,19]

$$\alpha_{\mathrm{S}}(\nu-\nu_0) = \alpha_{\mathrm{D}}(\nu-\nu_0)\left[1+\frac{G}{2}\left(1+\frac{\Gamma^2}{(\nu-\nu_0)^2+\Gamma^2}\right)\right]^{-1} \tag{6}$$

where $\alpha_{\mathrm{D}}(\nu-\nu_0)$ is the line shape of the Doppler-broadened background discussed earlier, Γ is the width (FWHM) of the Lamb dip and G, proportional to $I(\nu)/I_{\mathrm{S}}(\nu_0)$ (denominator denotes the saturation intensity), is a measure of the degree of saturation. Figure 5 shows the residual of the observed and simulated spectra. It may be noted that this transition consists of six lines including the crossover components, having a maximum frequency separation of nearly 30 MHz between the successive transitions. However, small residual and excellent fit of the spectrum with one transition centred at the unsaturated line frequency exhibits complete overlap of all transitions at this resolution. Table 2 contains the values of the saturation parameter (G) and Γ (FWHM) obtained by non-linear least squares fit of the observed line shape with the simulated profile mentioned in Eq. (4) for the three different laser powers. The increase of laser power enhances the intensity of the Lamb dip profile (Fig. 5) at the cost of its broadening. The measured linewidth Γ at different powers include the contributions of the unresolved hyperfine components of all six transitions. For an increase of laser power by 3.2 mW, the linewidth (Γ) increases by 3.56 MHz at ambient temperature. This indicates power broadening of nearly 1 MHz/mW.

TABLE 2. Values of saturation parameter, G, and power broadened linewidth (FMHM) Γ for the ^{85}Rb $F_g = 2 \rightarrow F_e$ transition, for three laser powers. The numbers in parentheses are one standard deviations in units of least significant digits.

Power (mW)	G	Γ (FWHM) (MHz)
1.9	0.588(29)	44.21(25)
3.5	0.985(68)	45.99(21)
5.1	1.521(51)	47.87(39)

4. *Conclusion*

Temperature dependent measurement of Rb D_2 transitions leads to the velocity estimation of vapour atoms from measured linewidths in the ambient temperature region along with the determination of line intensity. The line shapes for free-running temperature and steady-state temperature are identical, showing fast thermal equilibration of all atoms. Power-dependent measurements lead to the saturation parameter for the ^{85}Rb transition, which has not been reported earlier. The natural linewidth preponderates over other mechanisms.

The fully resolved saturated-absorption spectra of the ^{87}Rb D_2 transitions show the linewidths (HWHM) varying between 10 and 15 MHz (Fig. 6). The natural linewidth, power broadening, transit-time broadening and the laser linewidth with the instrumental contribution together lead to the linewidth (HWHM) of the order of 10 MHz. Akulshin et al. [21] measured the power-broadened linewidth of the crossover resonance of ^{85}Rb D_2 transition in a Doppler-free condition with chopper modulation technique. They did not report the variation of linewidth of hyperfine components. We recorded the hyperfine components using source-modulation technique which enhances the sensitivity of the measuring system. This enhanced sensitivity of the system allows measurement of the variation of linewidths of hyperfine components. The observed variation of HWHM of different hyperfine components may be explained as a small variation in the spontaneous decay rates of the excited-level populations in the presence of the saturating field. For optical transitions between one lower level and three closely spaced upper levels, the incoherent decay of the excited-level populations among themselves may also be significant in comparison to their spontaneous decay. In case of ^{85}Rb D_2 transitions, the hyperfine components of the transition $F_g = 3 \rightarrow F_e = 2, 3, 4$ could be partially resolved while the components $F_g = 2 \rightarrow F_e = 1, 2, 3$ did not show any structure. This is due to the smaller splitting of the hyperfine levels. This may also arise if the Rabi frequency is larger than the separation of excited levels [22], leading to larger power broadening along with weaker incoherent decay of the upper-level populations, resulting in hyperfine level-coupling effect at high laser power [23]. Also the saturation power may be lowered for the hyperfine optical-pumping effects in the three or higher-level alkali atoms compared to that in the two-level systems [20,24], giving rise to larger broadening of the lines. A detailed theoretical study of the complete line shape with one lower level and three closely spaced upper levels, with the aim to explain the observed line shape, is in process and will be published elsewhere.

Acknowledgements

D. B. and B. K. D. thank the Council of Scientific and Industrial Research, New Delhi, for research fellowships. Financial assistance from the Department of Science and Technology (SP/S2/L-05/96), New Delhi, is gratefully acknowledged.

References

[1] C. E. Wieman, G. Flowers and D. Gilbert, Am. J. Phys. **63** (1995) 317.

[2] M. H. Anderson, J. R. Ensher, M. R. Mathews, C. E. Wieman and E. A. Cornell, Science **269** (1995) 198.

[3] K. B. McAdam, A. Steinbach and C. E. Wieman, Am. J. Phys. **60** (1992) 1098.

[4] O. Trinks and W. Beck, Appl. Opt. **37** (1998) 7070.

[5] V. Mahal, A. Arie, M. A. Arbore and M. M. Fejer, Opt. Lett. **21** (1996) 1217.

[6] J. Ye, S. Swartz, P. Jungner and J. L. Hall, Opt. Lett. **21** (1996) 1280.

[7] J. C. Camparo, Contemp. Phys. **26** (1985) 443.

[8] C. Corsi, F. D. Amato, M. De Rosa and G. Modugno, Eur. Phys. J. D **6** (1999) 327.

[9] B. Ray and P. N. Ghosh, Spectrochim. Acta A **53** (1997) 537.

[10] B. K. Dutta, D. Biswas, B. Ray and P. N. Ghosh, Eur. Phys. J. D **11** (2000) 99.

[11] B. K. Dutta, D. Biswas, B. Ray and P. N. Ghosh, Eur. Phys. J. D **13** (2001) 337.

[12] A. Bruner, A. Arie, M. A. Arbore and M. M. Fejer, Appl. Opt. **37** (1998) 1049.

[13] S. E. Park, H. S. Lee, T. Y. Kwon and H. Cho, Opt. Commun. **192** (2001) 49.

[14] V. S. Letokhov and V. P. Chebotayev, *Nonlinear Laser Spectroscopy*, Springer-Verlag, Berlin (1977).

[15] W. Demtröder, *Laser Spectroscopy*, Springer-Verlag, Berlin (1982).

[16] H. Tsuchida, M. Ohtsu, T. Tako, N. Kuramochi and N. Oura, Jpn. J. Appl. Phys. **21** (1982) L561.

[17] P. R. Bevington, *Data Reduction and Error Analysis for Physical Sciences*, McGraw Hill, New York (1969).

[18] K. Shimoda, *High-Resolution Laser Spectroscopy*, Springer-Verlag, Berlin (1976).

[19] A. Corney, *Atomic and Laser Spectroscopy*, Clarendon Press, Oxford (1977).

[20] U. Tanaka and T. Yabuzaki, Jpn. J. Appl. Phys. **33** (1994) 1614.

[21] A. M. Akulshin, U. A. Sautenkov, V. L. Velichansky, A. S. Zibrov and M. V. Zverkov, Opt. Commun. **77** (1990) 295.

[22] S. Mandal and P. N. Ghosh, Phys. Rev. A **45** (1992) 4990.

[23] P. N. Ghosh and S. Mandal, Chem. Phys. Lett. **164** (1989) 279.

[24] T. Yabuzaki, T. Endo, M. Kitano and T. Ogawa, Opt. Comm. **22** (1977) 181.

SPEKTROSKOPSKA MJERENJA PRIJELAZA D_2 Rb U OVISNOSTI O TEMPERATURI I SNAZI SA I BEZ DOPPLEROVOG EFEKTA

Pomoću diodnog lasera s vanjskim rezonatorom načinili smo mjerenja oblika linija prijelaza D_2 Rb. Mjerenja temperaturne ovisnosti fine strukture izveli smo u uvjetima slobodno promjenljive temperature, upotrebom frekventne rampe za ponavljanje struje, podešene za područje 17 GHz koje obuhvaća sva četiri Dopplerovim efektom proširena prijelaza dvaju izotopa Rb u uvjetima gotovo bez sudara. Širenje linija Dopplerovim efektom u ovisnosti o temperaturi, utvrđeno metodom najmanjih kvadrata, daje korijene iz srednjih kvadrata brzina atoma u parama. Spektroskopska mjerenja sa zasićenom apsorpcijom pokazuju potpuno razlučivanje hiperfinih Lambovih i preskočnih rezonantnih minimuma prijelaza D_2 ^{87}Rb. Podatke iz mjerenja ovisnosti o snazi za nerazlučeni prijelaz D_2 ^{85}Rb smo analizirali radi dobivanja parametara zasićenja i koeficijenta širenja sa snagom. Širine potpuno razlučenih linija hiperfinih Lambovih i preskočnih rezonantnih minimuma nisu jednake, što ukazuje na različitost njihovih prirodnih širina.